# REPORT DOCUMENTATION PAGE

Form Approved OMB No. 0704-0188



| 1. AGENCY USE ONLY (Leave blank) | 2. REPORT DATE | 3. REPORT TYPE AND DATES COVERED |
|---|---|---|
| | 2 ~~December~~ OCT 99 | Final Report |

**4. TITLE AND SUBTITLE**

Ultrafast Optical Processing

**5. FUNDING NUMBERS**

F61775-98-WE055

**6. AUTHOR(S)**

Dr. Anatoly Grudinin

**7. PERFORMING ORGANIZATION NAME(S) AND ADDRESS(ES)**

University of Southampton
Southampton SO9 5NH
United Kingdom

**8. PERFORMING ORGANIZATION REPORT NUMBER**

N/A

**9. SPONSORING/MONITORING AGENCY NAME(S) AND ADDRESS(ES)**

EOARD
PSC 802 BOX 14
FPO 09499-0200

**10. SPONSORING/MONITORING AGENCY REPORT NUMBER**

SPC 98-4029

**11. SUPPLEMENTARY NOTES**

**12a. DISTRIBUTION/AVAILABILITY STATEMENT**

Approved for public release; distribution is unlimited.

**12b. DISTRIBUTION CODE**

A

**13. ABSTRACT (Maximum 200 words)**

This report results from a contract tasking University of Southampton as follows: The contractor will demonstrate data header erasure at 500 gigabits per second and investigate the ultimate speed of the nonlinear intensity modulator based on the Raman effect. Two approaches will be considered to study the ultimate performance of the Raman intensity modulator. First, to study the nonlinear and photorefractive properties of recently developed optical glass materials. Second, to study a complex structure comprising a D-shaped silica fiber with a thin lay of highly nonlinear semiconductor deposited on the flat surface of the fiber. The research will consider optical loss, polarization, and photorefractive sensitivity of the structure.



**14. SUBJECT TERMS**

EOARD, Fibre Optics, Optoelectronic materials, Optoelectronic components

**15. NUMBER OF PAGES**

17

**16. PRICE CODE**

N/A

| 17. SECURITY CLASSIFICATION OF REPORT | 18. SECURITY CLASSIFICATION OF THIS PAGE | 19. SECURITY CLASSIFICATION OF ABSTRACT | 20. LIMITATION OF ABSTRACT |
|---|---|---|---|
| UNCLASSIFIED | UNCLASSIFIED | UNCLASSIFIED | UL |

# Ultrafast Optical Processing

**A. B. Grudinin**

*Optoelectronics Research Centre*
*University of Southampton*
*Southampton SO17 1BJ*
*UK*

**Final Report submitted to**
**European Office of Aerospace Research and Development**
**(EOARD)**
**Contract F61775-98-WE055**

**October, 1999**

## I. Introduction

As telecommunication technologies mature there has been a drive towards all-optical transparency without the need of optical-to-electrical conversion. In particular, often at nodes within a telecommunications system a data header has to be erased and re-written for routing purposes. Currently, the approach is based on detection of the incoming data signal, its demodulation, and then after rewriting the appropriate header data to retransmit the packet or ATM cell. In future systems striving for all-optical transparency, an alternative approach is to use electro-optical modulators capable of operating at bit-rate frequencies. Commercial Mach-Zehnder modulators, currently built in $LiNbO_3$, can operate at 10 Gb/s and most likely will reach 40 Gb/s using traveling wave electrode structures; other electro-optic materials including GaInAs modulators may be capable of reaching 100 Gb/s [1]. However, this performance may be insufficient for future bit-rate transparent TDM systems that may require nodes to process data at bit rates in excess of 100 Gb/s. In this paper we demonstrate an all-optical header eraser at 10 Gb/s. Although only demonstrated at 10 Gb/s (limited by the laser pulse used in the experiments), the concept is based on the Raman effect with a response time shorter than 10 fs in silica fibers and should therefore be capable of operating at bit rates in excess of 500 Gb/s - ultimately limited by higher order nonlinear effects.

The proposed modulator originates from the well-known effect of signal depletion due to Raman gain [2, 3]. Thus, if data signals, which can be either a cw signal or pulses, and 'eraser' pulses are separated in wavelength by the Stokes shift, and co-propagate within telecommunication fibre then nonlinear interaction will lead to data signal attenuation that is proportional to the Stokes pulse intensity and to the interaction length of the two signals within the fibre. Typically, for Stokes power of order of 1 kW a Raman induced signal loss of ~4 dB/m can be realised. Because the data signal group velocity is greater, the data signal travels through the Stokes pulses transferring energy to them and thus creating a hole with width proportional to the interaction length, group velocity difference and wavelength separation. The erasure time window is about 1.5 ps/m for a fibre dispersion of 17 ps/nm·km, and data signal and Stokes separation of ~100 nm. [4]

In this report we present both theoretical and experimental study of ultimate limits of the proposed nonlinear modulator.

Since the operational principle of the modulator is based on nonlinear effects in optical fibers let us consider fibre nonlinearity in some more details.

## II. Nonlinear effects in optical fibres

The response of an optical fibre to light becomes non-linear for intense optical fields. On a fundamental level, the origin of the nonlinear response is related to the anharmonic motion of bound electrons under the applied field. Thus, the induced polarisation **P** becomes a non-linear function of the applied field **E** and may be written as

$$\mathbf{P} = \varepsilon_0(\chi^{(1)} \cdot \mathbf{E} + \chi^{(2)}:\mathbf{EE} + \chi^{(3)}:\mathbf{EEE}), \tag{4}$$

where $\varepsilon_0$ is the vacuum permittivity and $\chi^{(I)}$ is the i-th order susceptibility. The linear susceptibility $\chi^{(1)}$ represents the main contribution to P. Its effects are included through the refractive index and attenuation coefficient. The second-order susceptibility accounts for second harmonic and sum-frequency generation which normally do not exist in optical fibres.

The lowest-order nonlinearity in optical fibres originates from the third-order nonlinearity and results in self-phase modulation, third-harmonic generation, four wave mixing , Raman and Brillouin scattering.

### a) Self-phase modulation and modulation instability in optical fibres

The existence of $\chi^{(3)}$ means that the medium (i.e. glass) has a refractive index which is proportional to the optical intensity $|E|^2$ and this otherwise small effect becomes noticeable at high illumination. Under intense illumination refractive index can be presented as

$$n(\omega,|E|^2) = n(\omega) + n_2|E|^2, \tag{5}$$

where $n(\omega)$ is the linear part and $n_2$ is the non-linear coefficient related to $\chi^{(3)}$ by the expression

$$n_2 = \frac{3}{8n}\mathrm{Re}(\chi^{(3)}). \tag{6}$$

Here Re represents the real part and the optical field is assumed to be linearly polarised. In practice however, very often the polarisation is completely scrambled which reduces the effective non-linear refractive index. In silica $n_2$ is dominated by the electronic contribution , so to a good approximation we can write [2]

$$(n_2|E|^2)_{\text{average}} = \frac{5}{6}(n_2|E|^2)_{\text{linear}}. \tag{7}$$

The intensity-dependent refractive index leads to an intensity-dependent phase of the propagating wave, i.e.

$$\phi(t,|E|^2) = knz = k(n_0 + n_2|E|^2)z = \phi_{\text{lin}} + \phi_{\text{nl}}, \tag{8}$$

where $k=2\pi/\lambda$ is the wave-number. In practical computations it is more convenient to use light intensity rather than electrical fields so that Eq.(7) may be written in the form

$$\phi_{nl} = kn_2Iz \tag{9}$$

and we can define a nonlinear length $z_{nl}$ as

$$\phi_{nl} = kn_2Iz_{nl} = 1 \tag{10}$$

or

$$z_{nl} = (kn_2I)^{-1} \tag{11}$$

where I is the light intensity in $W/cm^2$ and $n_2=2.6\cdot10^{-16}cm^2/W$. Such a small value of the non-linear refractive index causes negligible changes in the value of the refractive index itself (even pulses with 100 kW peak power result in $\sim 4\cdot10^{-5}$ refractive index change which is approximately two orders of magnitude lower than the core-cladding refractive index difference).

The main effect caused by the non-linear refractive index is the generation of new spectral components due to self-phase modulation (SPM) i.e. spectral enrichment of the propagating pulses. This is because the non-linear phase given by Eq.(9) incurs a time-dependent variation of the instantaneous frequency $\omega$ that can be written as

$$\omega = \omega_0 + \frac{\partial\phi_{nl}}{\partial t} = \omega_0 + kn_2z\frac{\partial I}{\partial z} \tag{12}$$

or

$$\omega - \omega_0 = kn_2z\frac{\partial I}{\partial t}. \tag{13}$$

Thus the shorter the pulses and the higher their intensity the greater the spectral enrichment due to SPM. The most interesting and important consequence of SPM is not spectral broadening itself but nonlinear interaction of the spectral components in a pulse due to group velocity dispersion. If we consider an optical pulse propagating down the fibre (Fig.1 a) then SPM results in a frequency distribution whereas lower frequencies are gathered on the leading edge of the pulse, while higher frequencies are mainly situated at the trailing edge, as it shown on Fig.1b.

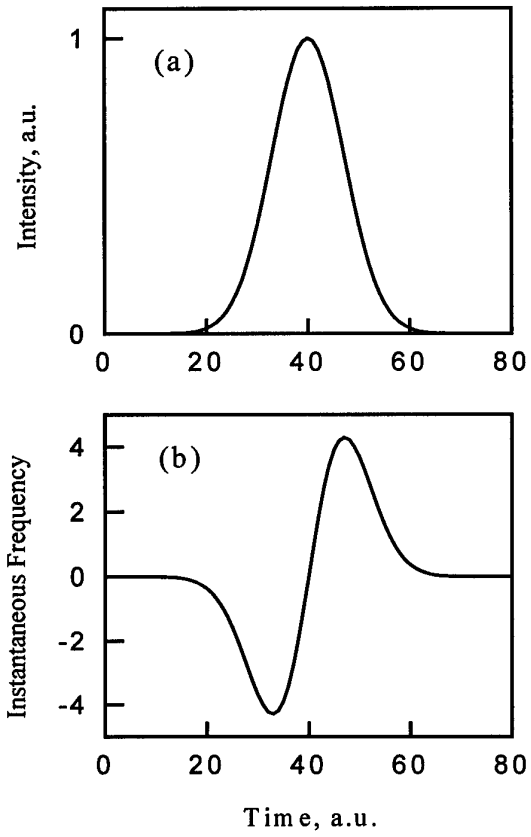


*Fig. 1 Effect of self-phase modulation, showing the pulse shape (a) and the instantaneous frequency deviation of the spectral components (b)*

It is quite obvious that if the pulse propagates in a medium where lower frequencies travel faster than higher ones (i.e. normal dispersion which typically corresponds to $\lambda < 1.3\mu m$ in standard telecom fibres), SPM would result in additional pulse broadening and after some distance the pulse shape would look like shown in Fig.2b.

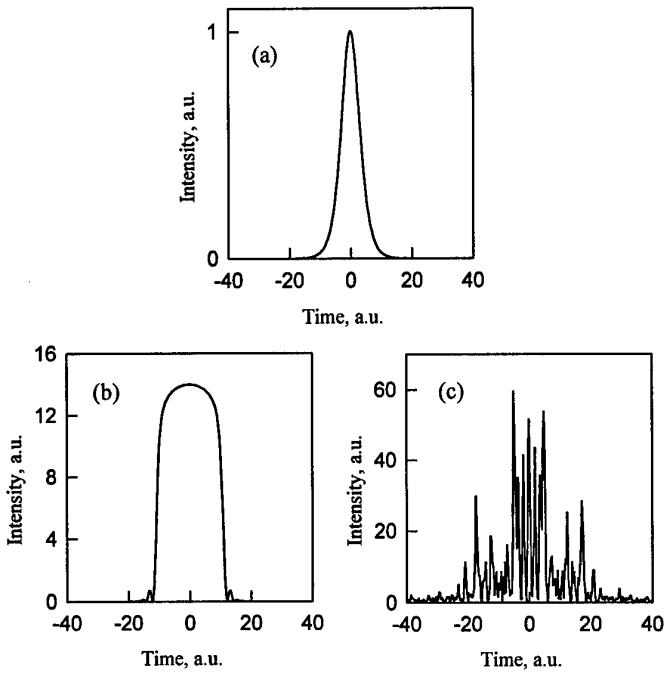


*Fig.2 Effect of combined action of fibre nonlinearity and dispersion. Profiles of the original pulse (a) and after travelling in fibre with normal (b) and anomalous dispersion (c)*

If however the pulse propagates in the region with anomalous dispersion ($\lambda > 1.3$ μm) then "blue" components travel faster then "red" ones and move from the trailing edge of the pulse to its leading edge so the pulse starts to reduce its temporal width and this is the so called soliton effect.

In order to get some feeling what sort of peak power one needs to observe this nonlinear compression, we need to compare two characteristic lengths: the nonlinear length defined by Eq.(10) and the dispersion length, which can be written as

$$z_d = \frac{2\pi c\tau^2}{(1.76\lambda)^2 D} . \qquad (14)$$

where D is the fibre dispersion and c is the speed of the light. Intuitively it is clear that the dispersion and nonlinearity balance each other when the two characteristic lengths are equal and doing so we have

$$I = \frac{(1.76\lambda)^2 D}{2\pi c k n_2 \tau^2} \qquad (15)$$

If now we take the fibre cross section to be $A_{eff} = 50\ \mu m^2$ then we arrive at a very simple relation between the parameters of the fibre and the propagating pulse

$$P_{peak} \approx \frac{D\lambda^3}{2\tau^2}, \tag{16}$$

where $P_{peak}$ is in Watts, D is in ps/nm·km, $\tau$ is in ps and $\lambda$ is in μm. So if one operates near 1.55 μm, then just 300 mW peak power is required to observe soliton effects for 10 ps pulses.

The situation becomes slightly more complicated when the pulsewidth increases, because in accordance with Eq.(16) the peak power decreases as the square of the pulsewidth and theoretically for 10 ns pulses soliton effects should be observed at nW levels. Usually, this does not happen mainly because 10 ns pulses are not bandwidth limited and the effective fibre length is limited to several kilometres while to observe non-linear effects at nW level one would need ~$10^7$ km of fibre.

However when a long (1ns-100 μs) high intensity (> 500 mW) pulse propagates in a fibre with anomalous dispersion it experiences nonlinear phase shift which results in the development of modulation instability. Modulation instability is a process in which the amplitude and phase modulations of a pulse grow as a result of interplay between the fibre nonlinearity and dispersion. It can be shown that the critical frequency of modulation instability (i.e. shortest pulsewidth which might be formed) can be written in the form [1]

$$0 < \Omega < \Omega_c = \left(\frac{kn_2 I}{k''}\right)^{1/2}, \tag{17}$$

where $k'' = D\lambda^2/(2\pi c)$ and $\Omega \sim 1/\tau$. Eq.(17) has actually a very simple physical meaning: as soon as the nonlinear length becomes shorter than the dispersion length, the pulse tends to compress or split into several individual pulses with dispersion length equal to or longer than the nonlinear length. It can also be shown [5] that if

$$N = (z_d / z_{nl})^{1/2} > 20 - 25 \tag{18}$$

then the propagating pulse tends to split into N individual pulses with random phases and nearly random amplitudes.

As an example let us consider a 100 ns pulse with 500 mW peak power propagating in a fibre with an effective cross-section of 50 $\mu m^2$ . From Eq.(18) one can see that for this pulse $N \approx 2 \cdot 10^4$ which means that after ~ 2 km a 100 ns 500 mW pulse evolves into noise-like burst of 0.1-1 ps pulses (see Fig. 2c).

**b) Four-wave mixing**

Four-wave mixing is a third order parametric process when three optical waves are involved in generation of fourth one. Mathematically the process may be presented in the form

$$E_4 \sim \chi^{(3)}[E_1E_2E_3\exp(i\Theta_+) + E_1E_2E_3\exp(i\Theta_-)] \quad (19)$$

where

$$\Theta_+ = (k_1 + k_2 + k_3 - k_4)z - (\omega_1 + \omega_2 + \omega_3 - \omega_4)t \quad (20a)$$

and

$$\Theta_- = (k_1 + k_2 - k_3 - k_4)z - (\omega_1 + \omega_2 - \omega_3 - \omega_4)t \quad (20b)$$

Four wave mixing is most effective when phases (20a and b) are equal to zero. This requires matching frequencies as well as wave numbers.

There are two types of four-wave mixing processes. Eq.(20a) describes the process when three waves with frequencies $\omega_1$, $\omega_2$ and $\omega_3$ transfer energy to the fourth wave at $\omega_4$ so that $\omega_4 = \omega_1 + \omega_2 + \omega_3$ (note that when $\omega_1=\omega_2=\omega_3$ this results in third harmonic generation).

The more important is the second case (20b), when two waves at $\omega_1$ and $\omega_2$ generate new components at $\omega_3$ and $\omega_4$ such that

$$\omega_1 + \omega_2 = \omega_3 + \omega_4 \quad (21)$$

Very often $\omega_1 = \omega_2$ and Eq.(21) may be re-written in the form

$$2\omega_p = \omega_s + \omega_a, \quad (22)$$

where indices p, s and a stand for pump, Stokes and anti-Stokes

The phase matching condition for this process can be written as

$$\Delta k = 2k_p - k_s - k_a = 2n_p\omega_p - n_s\omega_s - n_a\omega_a = 0 \quad (23)$$

and it can be shown [3] that this condition can be satisfied near the zero dispersion wavelength. However if the spectral width of the pulses is broad enough (~ 10 nm), then this effect does not result in any significant spectral changes.

**c) Stimulated Brillouin Scattering**

Stimulated Brillouin scattering (SBS) is a nonlinear process which manifests itself through the generation of a backward-propagating Stokes wave. In silica the central frequency of the Stokes wave is shifted by ~ 10 GHz from the central wavelength of the pump signal. The gain coefficient is about $10^{-9}$ cm/W i.e. two orders of magnitude higher than the Raman gain. However, if the spectral width of the pump pulse exceeds 10 GHz then the Brillouin gain reduces by a factor

$$\eta = \frac{\Delta\nu_b + \Delta\nu_s}{\Delta\nu_b} \approx \frac{\Delta\nu_s}{\Delta\nu_b} \quad (24)$$

i.e. becomes comparable with the Raman gain for light with spectral width of 10 nm pulses. However, since Brillouin scattering is most efficient in the backward direction

then the interaction length of pump and Stokes waves is defined by their overlap which equals to the spatial length of the probe pulse. Even for 10 μs pulses this does not exceed 2 km and the nonlinear gain associated with Brillouin scattering is therefore an order of magnitude lower than the Raman gain for co-propagating waves.

**d) Stimulated Raman scattering**

This is most important effect for the proposed nonlinear modulator.

When a high-intensity pump pulse propagates down the test fibre a small fraction of the pulse energy is frequency downshifted owing to scattering of the incident photons by molecules that make a transition between two vibrational states. Thus incident light acts as a pump for generating frequency-shifted radiation called the Stokes wave. The Raman gain coefficient g is related to the cross-section of spontaneous Raman scattering and has been measured experimentally in silica fibres in the early seventies [4].

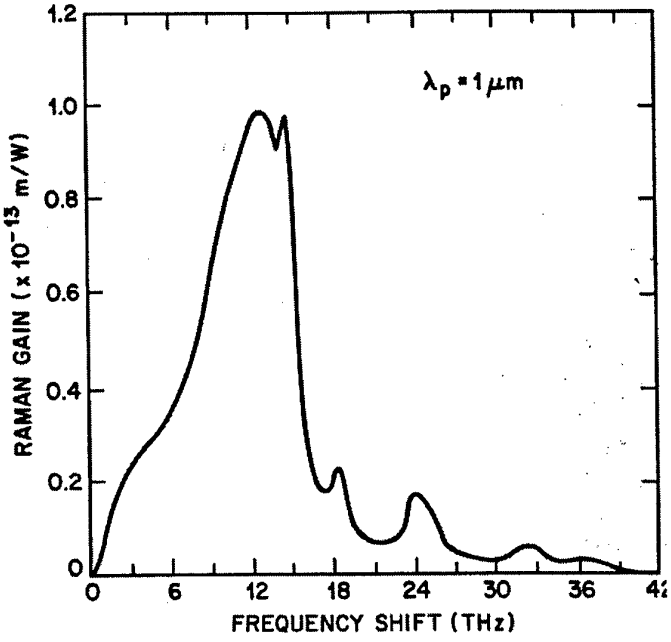


*Fig.3 Raman gain curve in silica glass [4]*

Fig.3 shows g for silica glass as a function of the frequency shift at a pump wavelength of 1 μm [4]. Near this wavelength $g \approx 10^{-11}$ cm/W. Due to its nature the Raman gain coefficient is inversely proportional to the pump wavelength i.e. its approximately 1.5 times lower at 1.55 μm than at 1μm.

Stimulated Raman scattering is a cascade process whereby a pump signal excites the first Stokes wave which in turn acts as a pump for a second Stokes component and so on. Fig.4 shows the development of SRS in a single mode fibre with pump at 1064 nm.

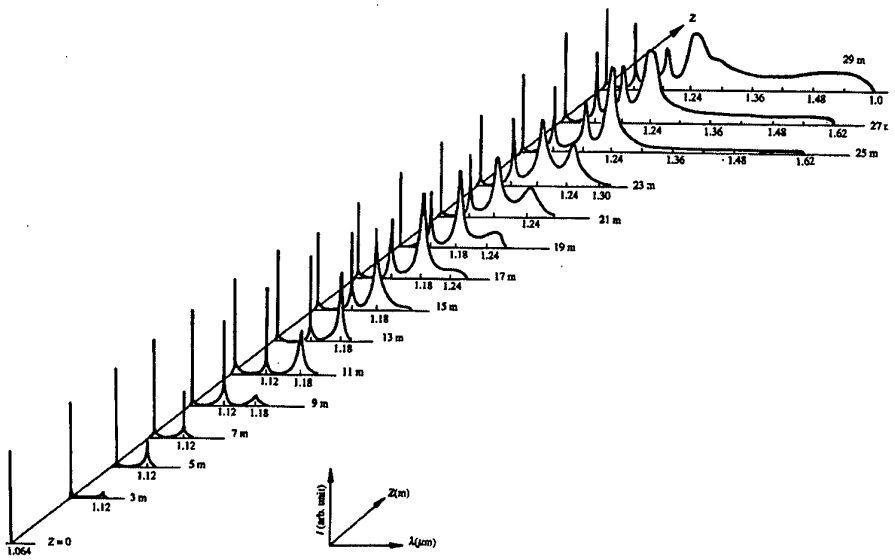


*Fig.4 Dynamics of SRS in a standard telecom fibre with $\lambda_0$ near 1320 nm [5]*

An interesting feature of the presented spectra is that there are three well-distinguished components situated at 1120, 1180 and 1240 nm and a very broad spectral continuum after the wavelength of zero group-velocity dispersion (~ 1320 nm). This fact has a simple explanation. The first three Stokes components are situated in the region of normal dispersion, so that the fibre nonlinearity and dispersion do not result in the formation of short nonlinear pulses via modulation instability. Moreover the interaction length is long enough for development of high intensity Stokes components. However, the fourth Stokes component is situated in the region of anomalous dispersion and the effect of modulation instability results in the formation of a burst of short (< 0.1 ps ) pulses with broad spectrum, that in combination with the Raman effect, lead to the formation of a spectral continuum [5].

To describe pulse propagation in the presence of Raman gain, one should consider the following set of non-linear differential equations

$$\frac{\partial u_p}{\partial z}+\frac{1}{v_p}\frac{\partial u_p}{\partial t}+\frac{i}{2}\beta_p''\frac{\partial^2 u_p}{\partial t^2}+i\gamma|u_p|^2u_p=-i\Gamma u_p+2i\gamma|u_s|^2u_p-g|u_s|^2u_p \qquad (25.a)$$

$$\frac{\partial u_s}{\partial z}+\frac{1}{v_s}\frac{\partial u_s}{\partial t}+\frac{i}{2}\beta_s''\frac{\partial^2 u_s}{\partial t^2}+i\gamma|u_s|^2u_s=-i\Gamma u_s+2i\gamma|u_p|^2u_s+g|u_p|^2u_s \qquad (25.b)$$

where $u_p$ and $u_s$ are pump and Stokes optical fields, $v_p$ and $v_s$ their group velocities, $\beta_p''$ and $\beta_s''$ are group velocity dispersions at pump and Stokes wavelengths respectively, $\gamma$ and g are nonlinear coefficients and $\Gamma$ is the fibre loss. The left-hand side is a standard non-linear Schrödinger equation while the first term on the right-hand side describes the

fibre loss, the second stands for the cross-phase modulation between pump and Stokes waves and the last term describes the Raman gain. Note that the energy conservation law requires pump depletion and this effect is taken into account by the last term in Eq.(25.a). The set of equations (25) can not be solved analytically owing to their complexity and a numerical method known as the split-step Fourier method is usually employed for numerical simulations on a personal computer. Below we present results of such computer simulations, but before doing so let us consider several simple cases that reveal major trends in stimulated Raman scattering. Firstly, we make two assumptions:

-the temporal width of the probe pulse is broad and therefore we neglect pulse broadening;

- the spectral width of the probe pulse is also broad and the effect of self-phase modulation need not be taken into account.

Now let us consider the effect of group-velocity mismatch between pump and Stokes waves. To do so let us consider again a pair of coupled equations for pump and Stokes waves:

$$\frac{\partial I_p}{\partial z}+\frac{1}{v_p}\frac{\partial I_p}{\partial t}=0$$
$$\frac{\partial I_s}{\partial z}+\frac{1}{v_s}\frac{\partial I_s}{\partial t}=gI_pI_s \qquad (26)$$

where $v_p$ and $v_s$ are the group velocities of pump and Stokes waves respectively.
The solution of (26) may be written as

$$I_p(\tau - z\Delta) = I_p(\tau - z/v) = I_p(0)\exp[-\frac{4(t-z/v)^2}{\tau_0^2}] \qquad (27.a)$$

and

$$I_s(\tau,z) = I_s(0)\exp[gI_p(t-z/v_p)z] \qquad (27.b)$$

where $\tau = t - z/v_s$ is running time, $\Delta = 1/v_p - 1/v_s = 1/2(D_p + D_s)\Lambda$, $D_p$ and $D_s$ are the chromatic dispersion at the pump and Stokes wavelengths respectively and $\Lambda = \lambda_p - \lambda_s$.

If we assume that the Stokes waves start from spontaneous noise, then in order to make the Stokes signal comparable to the pump, one needs gain G of the order of 20 and we define it as the threshold gain i.e.

$$G_{th} = 20 \qquad (28)$$

Now let us consider the experimental situation when a high intensity pump pulse propagates down the test fibre. A pair of coupled equations for pump and Stokes waves, $I_p$ and $I_s$ respectively can be written in the form

$$\frac{dI_p}{dz} = -\alpha I_p - \frac{\omega_p}{\omega_s}g(z)I_pI_s, \qquad (29)$$

and

$$\frac{dI_s}{dz} = -\alpha I_s + g(z) I_p I_s \tag{30}$$

where the second term on the RHS of Eq.(35) describes pump depletion due to SRS, while the second term on the RHS of Eq.(36) represents Raman gain.

If we combine two equations (35 and 36) then

$$\frac{dI_s}{dz} = -\alpha I_s + g(z) I_s I_p(0) \exp(-\alpha z). \tag{31}$$

This equation has the obvious solution.

$$I_s(z) = I_{sp} \exp(-\alpha z) \exp[I_p(0) \int_0^z g(z) \exp(-\alpha z) dz]. \tag{32}$$

Note, that if g(z)= const, then we have

$$\int_0^z \exp(-\alpha z) dz = \frac{1}{\alpha}[1 - \exp(-\alpha z)]. \tag{33}$$

Optical loss results in energy dissipation and it is convenient to introduce an effective length $z_{eff}$, defined as

$$z_{eff} = \frac{1 - \exp(-\alpha z)}{\alpha}. \tag{34}$$

The interpretation of $z_{eff}$ is that in a fibre with loss, the pump and Stokes waves interact over a limited distance given by Eq.(40).

## III. Raman modulator operating in soliton regime

Let us now explore ultimate limits of the Raman modulator.

The extinction ratio of the proposed intensity modulator is defined by intensity of the Stokes pulse and the interaction length between the Stokes and signal pulses. For 20 dB of extinction ratio one needs gIz = 4.6, where g is the Raman gain coefficient in silica fibre (~ $5 \cdot 10^{-12}$ W/cm @ 1550 nm), I is intensity of the Stokes pulses and z is the interaction length.

The speed of the modulator is defined by the pulsewidth of the Stokes pulse and walk-off between the Stokes and signal pulses. Thus for a modulator operating at 1 THz one needs pulses as short as 1 ps. Let us now consider how this modulator works and what effects might (and will) affect the maximum achievable speed of this device.

Operating in the region of 1550 nm is almost inevitable to use optical solitons. It is straightforward to demonstrate that without walk-off effect extinction ration achieved with a fundamental soliton over one soliton period would be

$$\eta = 4.3 \frac{g\lambda}{4n_2} \approx 4.3 \text{ dB}. \tag{35}$$

Note that extinction ratio is independent on the pulsewidth, fibre dispersion and almost independent on wavelength since $g\lambda \approx$ const in silica glass [2]. Thus to obtain 20 dB extinction ratio one needs a fibre length equal to 5 soliton periods. Group velocities of the Stokes and signal should be equal (to avoid walk-off between two interacting waves) and it suggests the use of a fibre with flat dispersion curve in the region of 1.55-1.65 μm. Assuming dispersion of 1 ps/nm·km the fibre length should be in the region of 1.5 km.
The long fibre length results in long latency (~ 7.5 μs) and this in some cases may be intolerable.
Another obvious way to obtain the required extinction ratio is to increase the Stokes pulse intensity i.e. instead fundamental solitons to use multi-soliton pulses.
The required soliton number N to reach η dB extinction ratio over one walk-off length can be written in the form

$$N^2 = 0.23\eta\tau\frac{\pi c\Delta\lambda}{\lambda^2} \tag{36}$$

where $\Delta\lambda$ is the frequency shift between the Stokes and pump signals and Eq. (1) was taken into account. Note that number of solitons is independent of the fibre dispersion and proportional to the pulsewidth.
For a 1 ps pulses the soliton number is $N \approx 13$ and walk-off length $z_w=\tau/(D\Delta\lambda)$ is 60 cm assuming fibre dispersion of 17 ps/nm·km.
In order to prevent break-up of multi-soliton pulses compression length $z_c$ should be greater then walk-off length (or physical length of the nonlinear fibre modulator). In other words

$$z_c = \frac{z_0}{\pi N} > \frac{\tau}{D\Delta\lambda}, \tag{37}$$

and this expression imposes limit on pulsewidth. Combining Eqs.(2) and (3) one can obtain the following expression for the pulsewidth

$$\tau > 0.23\eta\frac{\pi^3\lambda^2}{4c\Delta\lambda}, \tag{38}$$

Thus for 20 dB of extinction ratio the Stokes pulsewidth should be greater than 2.7 ps, system latency is shorter then 13 ns and this intensity modulator will have maximum operating frequency of 250 -300 GHz.

## IV. Experimental results

In the experiment we have employed 2.1 ps pulses from passively mode-locked fibre laser operating at 1543 nm. The pulses after an optical amplifier were launched into a length of standard telecom fibre via a WDM. A low level (several mW) cw signal at 1480 nm was launched through another port of the WDM. Output signal (at 1460 nm) were taken by fast photodiode while temporal shape of Stokes pulses was measured in an intensity autocorrelator.
Peak power of the 2.1 ps Stokes pulses were 1.2 kW, fundamental soliton peak power was 7 W, soliton number N = 13 and walk-off length was 1.5 m.
First we taken data after 1.5 m of standard telecom fibre which are shown in Fig.5

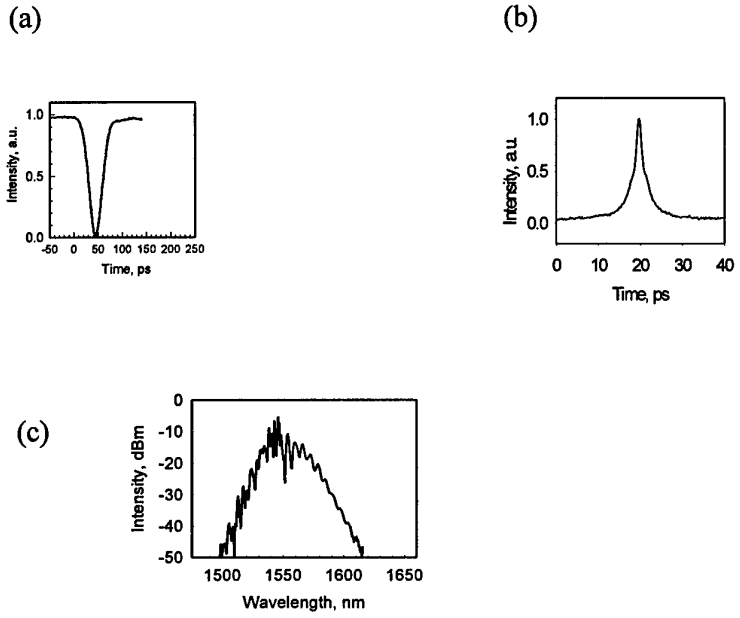


*Fig.5 Hole profile at signal wavelength (a) and temporal shape (b) and spectrum (c) of the Stokes pulse after 1.5 m of interaction length.*

As one can see interaction between signal and Stokes waves resulted in depletion of the signal. Temporal width of the hole is 30 ps and is limited by our detection system. The shape of the Stokes pulse at the output (Fig.5b) is similar to that at the input although some pulse narrowing has already taken place. Spectrally the Stokes pulse became much broader (Fig.5c).
Note that in present experimental arrangements we are unable to record the actual shape of the hole due relatively slow speed of the detection system. Our estimates indicate that the actual hole width is shorter then 6-8 ps and such narrow dark pulses can be detected using cross-correlation technique. When the fibre length was increased to 35 m the

situation has changed significantly. The hole width became 44 ps which corresponds to ~ 20 walk-off lengths (Fig.6a)

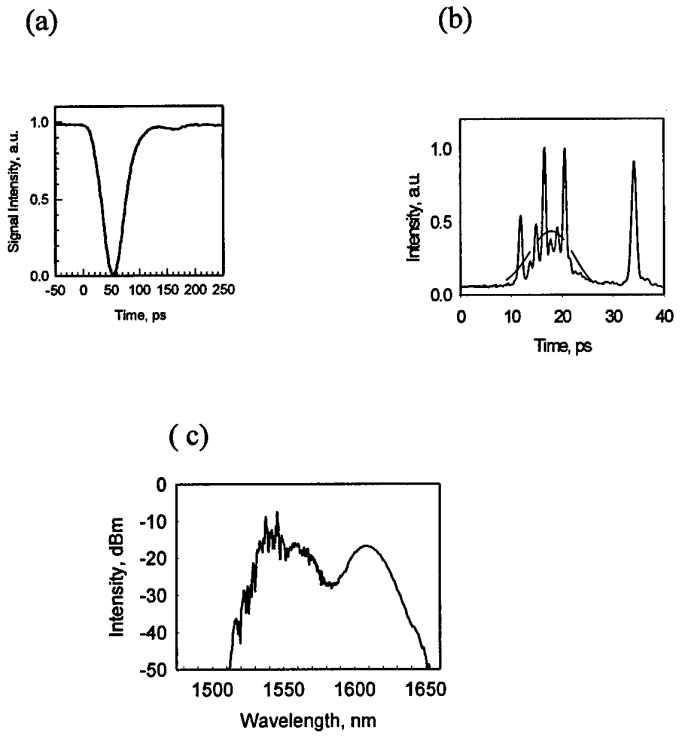


*Fig.6 The same as in Fig.1 but after 35 m of interaction length.*

In order to obtain temporal profile of the Stokes pulses at the output of the fibre we employed a cross correlation technique when the Stokes pulse was mixed with a reference sub-picosecond pulses at a nonlinear crystal. As one can see the Stokes pulse at the output end of the fibre broke up into several pulses (Fig.6b). Such instability of multi-soliton pulses is well known and it is quite clear that this effect restricts the length of the interacting fibre.

## V. Conclusion

Our theoretical and experimental results show that the ultimate speed of the intensity modulator based on the Raman effect is limited by the effect of self-phase modulation of Stokes pulses. Nevertheless it is feasible to achieve operation frequency in the region of 250 GHz which is almost order of magnitude higher than that offered by conventional modulators.

## VI. References


1. N. Dagli, University of California, Santa Barbara, private communication.
2. G.P. Agrawal, Nonlinear Fiber Optics, 2nd Edition, Academic Press, 1995
3. P. M. Kjeldsen, M. Øbro, J. S. Madsen and S. K. Nielsen, Electron. Letters, **32**, 1914, (1996)
4. R. H. Stolen, E. Ippen, Appl. Phys. Lett., **22**, 276 (1973)
5. Ch. 7 in *Optical solitons - theory and experiment*, ed. by J.R Taylor, Cambridge University Press, 1992
6. G. Burdge, S.-U. Alam, A. B. Grudinin, M. Durkin, M. Ibsen, I. Khrushchev and I. White, ECOC'97, Paper PD17 (1997)